Ureido-Based Peptidomimetic Inhibitors of Herpes Simplex Virus Ribonucleotide Reductase: An Investigation of Inhibitor Bioactive Conformation

Neil Moss,* Pierre Beaulieu, Jean-Simon Duceppe, Jean-Marie Ferland, Jean Gauthier, Elise Ghiro, Sylvie Goulet, Ingrid Guse, Montse Llinàs-Brunet, Raymond Plante, Louis Plamondon, Dominik Wernic, and Robert Déziel

Bio-Méga/Boehringer Ingelheim Research Inc., 2100 Cunard, Laval, Québec, Canada H7S 2G5

We have been investigating peptidomimetic inhibitors of herpes simplex virus (HSV) ribonucleotide reductase (RR). These inhibitors bind to the HSV RR large subunit and consequently prevent subunit association and subsequent enzymatic activity. This report introduces a new series of compounds that contain an extra nitrogen (a ureido function) at the inhibitor N-terminus. This nitrogen improves inhibitor binding potency 50-fold over our first published inhibitor series. Evidence supports that this improvement in potency results from a new hydrogen-bonding contact between the inhibitor and the RR large subunit. This report also provides evidence for the bioactive conformation around two important amino acid residues contained in our inhibitors. A *tert*-butyl group, which contributes 100-fold to inhibitor potency but does not directly bind to the large subunit, favors an extended β-strand conformation that is prevalent in solution and in the bound state. More significantly, the bioactive conformation around a pyrrolidine-modified asparagine residue, which contributes over 30 000-fold to inhibitor potency, is elucidated through a series of conformationally restricted analogues.

Introduction

We are currently exploring the use of peptidomimetic inhibitors of herpes simplex virus (HSV) ribonucleotide reductase (RR) as a potential treatment for herpes simplex infections. HSV RR plays a pivotal role in viral DNA biosynthesis by catalyzing the conversion of ribonucleoside diphosphates into the corresponding deoxyribonucleotides.[1] Our inhibitors act as mimics of the C-terminus of the HSV RR small subunit (R2). This C-terminal region binds to the RR large subunit (R1) thus enabling subunit association and subsequent catalytic activity.[2] Inhibition results from competitive binding of the inhibitors to R1 which prevents formation of the catalytically active holoenzyme. An attractive characteristic of this type of inhibition is that compounds based on the HSV R2 C-terminal sequence are selective for HSV RR over human RR.[3] Herpes and human RRs operate by the same mechanism and have similar structural features. However, the critical R2 C-terminal regions of these enzymes have little sequence homology; consequently, mimics of either enzyme's R2 C-terminus do not cross-inhibit the other ribonucleotide reductase.[4]

We recently reported that inhibitors of HSV RR subunit association could also prevent HSV replication in cell culture and reduce the severity of HSV-induced keratitis in a murine ocular model.[5] This work provided the first illustration that peptidomimetic compounds can prevent enzyme subunit association *in vivo*. In our continuing search for better HSV RR inhibitors, we have maintained an interest in improving inhibitor-binding potency. In this paper, we report a new structural modification that substantially improves inhibitor-bind-

ing potency over our first published inhibitor series[6] without significantly increasing inhibitor size.

We have also been trying to obtain information on the bioactive conformation of our peptidomimetic inhibitors. This information may eventually prove useful in the design of better inhibitors. At present no X-ray structural information exists for either subunit of HSV RR. An X-ray structure has been published for the *Escherichia coli* R1 bound to a peptide corresponding to the 20 C-terminal amino acids of the *E. coli* R2.[7] Although this fascinating structure reveals the binding mode of the *E. coli* C-terminal peptide, the information is not directly translatable to HSV RR. The R2 C-termini for *E. coli* and HSV have little sequence homology, and thus the binding modes are expected to be quite different.[4] Transferred NOE spectroscopy has been used to study the interaction between a peptide and *E. coli* R1.[8] Unfortunately, our attempts to apply this technique to HSV RR have proven unsuccessful. Thus, in the absence of structural information, we have instead deduced local inhibitor bioactive conformations by correlating inhibitory potency with the conformation of unbound inhibitors elucidated by NMR and molecular modeling. More importantly, we have also correlated potency with the structure of conformationally restricted inhibitors. We previously used this approach to provide evidence for the bioactive conformation of the aspartic acid region of our inhibitors.[9] Herein we describe how conformational restrictions have provided insight into the bioactive conformation of other important regions of our inhibitors.
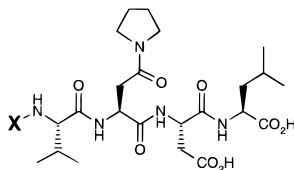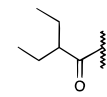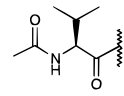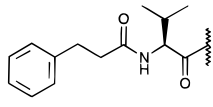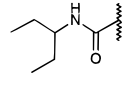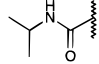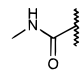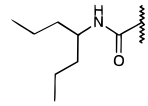
Results and Discussion

Ureido-Based Inhibitors. Early enzyme inhibition tests of peptides that corresponded to the C-terminus of the HSV R2 showed that the five C-terminal amino acids, Val-Val-Asn-Asp-Leu, contained the most important functionality for binding to R1.[10] We initiated
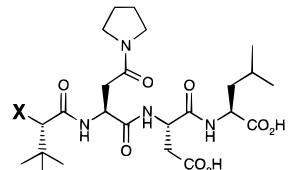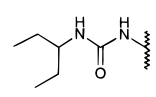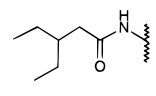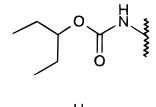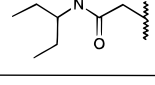
Table 1

Compound	X	Binding Assay IC_{50} (nM)
1		860 ± 240
2		880 ± 300
3		24 ± 5
4		15 ± 1
5		435 ± 37
6		$42\,000 \pm 4500$
7		7 ± 1

Table 2

Compound	X	Binding Assay IC_{50} (nM)
8		3 ± 0.5
9		140 ± 50
10		635 ± 95
11		5 ± 1

structure—activity studies based on this sequence. Compound **1** (Table 1) serves as a representative of our first published inhibitor series based on this initial investigation.[6] Compound **1** contains two significant modifications over the R2 C-terminal sequence. Firstly, the diethylacetyl N-terminus in compound **1** was found to effectively replace the N-terminal valine, and secondly, the replacement of the asparagine side-chain NH_2 with a pyrrolidine was shown to improve inhibitor-binding potency over 100-fold. We were initially attracted to the diethylacetyl N-terminus of compound **1** because it provided inhibitors equipotent to analogues containing the more peptidic *N*-acetylvaline N-terminus (e.g., compound **2**). Unfortunately, no inhibitor containing either the diethylacetyl or the *N*-acetylvaline N-terminus prevented viral replication in HSV cell culture. However, replacement of the acetyl group in compound **2** with a 3-phenylpropionyl group (compound **3**) increased binding potency over 30 times.[11] Compound **3** provided the starting point for structure—activity studies that led to the discovery of ribonucleotide reductase inhibitors effective at preventing HSV replication *in vitro* and *in vivo*.[5] The binding potency increase associated with the 3-phenylpropionyl group (illustrated by compound **3**) and related derivatives proved to be very important for inhibitor antiviral activity.

It is generally believed that smaller molecules stand a better chance of diffusing through biological membranes. Consequently, we have been conscious of identifying structural modifications that can improve binding potency without significantly increasing inhibi-

tor size. In this regard, we were delighted when we found that substituting the diethylacetyl N-terminus in compound **1** with an [(ethylpropyl)amino]carbonyl group (see compound **4**) increased inhibitor potency over 50-fold. This new modification provided a more potent inhibitor than the analogous compound containing the (phenylpropionyl)valine moiety (compound **3**) but with a molecular weight closer to that of compound **1**.

The fact that insertion of a NH group could have such a pronounced effect on binding potency intrigued us. Our previous structure—activity studies demonstrated that truncation of the N-terminal diethylacetyl group to an acetyl group in an inhibitor similar to compound **1** lowered binding potency over 1000-fold (compound inactive at 1000 μM).[6] We also knew that replacement of the N-terminal valine in compound **3** with glycine lowered potency ca. 5000-fold.[11] As it was evident that a lipophilic group at this position was essential for good inhibitor potency, we speculated that the N-terminal NH in compound **4** might serve to more favorably position the lipophilic group for binding to R1. However, sequential truncation of the (ethylpropyl)amino group in **4** to a methyl group (compounds **5** and **6**) culminated in a 2800-fold loss of potency. This potency loss corresponded to the potency loss observed with the other two inhibitor series. This argued against the NH group in compound **4** having a significant influence on the lipophilic binding interaction between the inhibitor N-terminus and R1. The strength of this lipophilic binding interaction could be augmented, however, by the addition of two methyl groups (*cf.* compounds **4** and **7**).

The compounds shown in Table 2 provide evidence that the N-terminal NH of this new ureido-based inhibitor series participates in a hydrogen-bonding interaction with R1. Replacement of this NH with a CH_2 lowers binding potency more than 40 times (*cf.* compounds **8** and **9**). More significantly, the corresponding carbamate analogue (compound **10**), which should impart similar geometrical constraints to the inhibitor as the ureido group in compound **8**, is 200
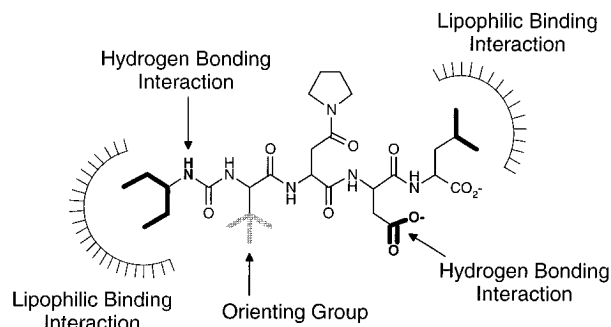
Figure 1.

times less potent. The N-terminal oxygen in compound **10** obviously cannot act as a hydrogen bond donor. The oxygen would not only be unable to partake in the same hydrogen-bonding interaction as the NH but may also face a repulsive interaction with the hydrogen bond acceptor on R1. This could explain the substantial potency difference observed. The hydrogen bond between the N-terminal NH of the urea-based inhibitors and R1 likely constitutes a novel binding interaction not utilized by the R2 C-terminus.

Unlike the N-terminal NH of the ureido group, the *tert*-leucine NH does not contribute significantly to binding potency. The similar IC_{50} values of compounds **8** and **11** indicate that the *tert*-leucine NH does not interact with R1 nor is it necessary for defining local inhibitor conformation.

It is also noteworthy that substituting the valine moiety in compound **4** (Table 1) with *tert*-leucine improves inhibitor-binding potency 5-fold (compound **8**, Table 2). This result is consistent with our previous findings. Replacement of the C-terminal valine with *tert*-leucine in compound **3** has also been shown to improve binding potency 5-fold.[11] This result demonstrates that the new ureido-based N-terminus is not influenced by the adjacent inhibitor functionality any differently than other N-terminal groups.

The significant potency increases obtained with this new urea-based N-terminus have of course encouraged us to investigate the effect of these inhibitors against HSV *in vitro* and *in vivo*. Incorporating previously published modifications at the inhibitor C-terminus into the ureido-based inhibitors does provide compounds with antiviral efficacy. Details regarding the antiviral properties of these urea-based inhibitors will be published in a separate account.

Investigation of Inhibitor Bioactive Conformation. Understanding an inhibitor's bioactive conformation and how the molecule binds to its target requires knowledge of what inhibitor functionalities are important for binding potency and why. Figure 1 uses compound **8** to summarize information learned from our first published structure–activity studies[6] and the previous section of this paper. The isopropyl group of the C-terminal leucine and the N-terminal pentyl group likely bind to lipophilic binding pockets on R1, while the aspartic acid carboxyl group probably participates in a strong hydrogen-bonding interaction. The absence of any one of these three groups causes over a 1000-fold loss in binding potency. Unlike the three previous groups, the *tert*-butyl group in compound **8** does not appear to interact directly with R1. Instead, it probably reduces conformational mobility in this region of the

Table 3

Compound	X	Binding Assay IC_{50} (nM)
8		3 ± 0.5
12		670 ± 150
13		240 ± 30
14		800 ± 170
15		41 000 ± 2500

inhibitor and helps favors a conformation which resembles the bioactive conformation. At this position, inhibitor potency improves with increased substitution of the amino acid β-carbon and is not strongly influenced by the type of functionality present.[6] On the basis of this information, we looked for the presence of predominant conformations around the inhibitor *tert*-butyl group in solution and investigated whether we could correlate this to the local bioactive conformation.

(a) Bioactive Conformation of *tert*-Leucine Residue. β-Branched amino acids such as valine and isoleucine are known to favor an extended peptide conformation (i.e., the peptide backbone conformation found in β-sheets).[12] It seems reasonable that *tert*-leucine would also favor this typical extended conformation, perhaps to a greater extent than valine or isoleucine. NMR coupling constants and NOE data for the *tert*-leucine portion of compound **8** and previously published inhibitors[9] (DMSO solution) show a relatively large H_a–H_b coupling constant (8.5–10 Hz) and a strong NOE between H_b and H_c (see compound **8** in Table 3).[13] These data are typical for an extended peptide conformation. Given that the conformation depicted in compound **8** (Table 3) appears to predominate in DMSO solution, we prepared conformationally restricted cyclic inhibitors to investigate if this conformation also resembles the bioactive conformation.

The strong NOE between H_b and H_c observed for compound **8** suggested mimicking the proximity of these two hydrogens by connecting the carbon and nitrogen atoms attached to H_b and H_c with a 5- or 6-membered ring. It was already known from a related inhibitor series that replacing H_c with a methyl group had little

effect on binding potency.[14] This implied that the H_c did not directly interact with R1 and thus would be amenable to structural modification. For synthetic simplicity, we prepared two cyclic analogues which lacked the *tert*-butyl group. These cyclic compounds were based on connecting the carbon and nitrogen atoms attached to H_b and H_c in glycine analogue **12** (see compounds **13** and **14**, Table 3). This simplification was justifiable even though the glycine analogue **12** lost over 200 times potency compared with the corresponding *tert*-leucine derivative **8**. As previously mentioned, this loss of potency is likely a consequence of increased inhibitor conformational mobility and not a consequence of a lost binding interaction. Compound **12** can still achieve the same peptide backbone conformation as compound **8**; however, compound **12** will populate many additional conformational states.

The 6-membered ring compound **13** is ca. 3 times more potent than the acyclic reference analogue **12**, while the 5-membered ring compound **14** is essentially equipotent. These conformational restrictions produce reasonably potent inhibitors and thus provide evidence that the close proximity of H_b and H_c observed for compound **8** in DMSO solution also exists in the bound state. Since, by design, the cyclic amino acids in compounds **13** and **14** have the unnatural *R*-configuration, we prepared the (*R*)-alanine derivative **15** as a further point of reference. The 50–170-fold difference between the (*R*)-alanine inhibitor **15** and compounds **14** and **13** more impressively exemplifies the suitability of these restrictions to approximate the optimal ψ angle for inhibitor binding (H_b–CO torsion angle). The modest potency of compound **13** compared to compound **8** is probably not a consequence of a nonoptimal ψ angle in **13**. More likely, the presence of the β-ring methylene in compounds **13** and **14** forces an unfavorable steric interaction with the adjacent urea carbonyl in the bound state. This would be predicted if the optimal ϕ angle for inhibitor binding is close to that shown in compounds **8** and **12** (H_a–H_b torsion angle around 180°). If one considers the 170-fold difference in potency between compounds **13** and **15** as a partial measure of how poorly the (*R*)-methyl group in **15** orients the adjacent C-terminal amide (ψ angle), it may be reasonable to assume that the (*R*)-alkyl groups in compounds **13**–**15** have a similar negative influence on the orientation of the adjacent urea (ϕ angle). Interestingly, this magnitude of potency difference is similar to the potency difference between compounds **8** and **13**.

(b) Bioactive Conformation of Pyrrolidine-Modified Asparagine Residue. The central amino acid side chain (asparagine modified with a pyrrolidine) contributes enormously to binding potency in all our inhibitor series. Replacement of this side chain with a methyl group can reduce binding potency over 30 000 times (*cf.* compounds **8** and **23**, Table 4). Our first structure–activity paper indicates that both the carbonyl group and the pyrrolidine (more specifically dialkylation of the side-chain nitrogen) contribute almost equally and independently to inhibitor potency.[6] However, it is not clear whether or to what extent these two side-chain functionalities engage in direct binding with R1 or contribute to favoring inhibitor bioactive conformation. As this central region of our inhibitors contributes so much to binding potency, we undertook an

Table 4

Compound	X	Binding Assay IC_{50} (nM)
8		3 ± 0.5
16		32 ± 6
17		3000 ± 800
18		10 ± 1
19		35 ± 3
20		108 ± 23
21		750 000 ± 90 000
22		100 000 ± 12 000
23		110 000 ± 16 000

investigation to gain information about this important region through studying its bioactive conformation.

NMR data from previously published inhibitors[9] provided information on the solution conformation (DMSO) of the pyrrolidine-modified asparagine moiety. The most distinctive piece of information was the relatively large and small coupling constants observed between H_d and H_e (9–11 Hz) and H_d and H_f (4–5 Hz), respectively (see Figure 2). These data are typical for a
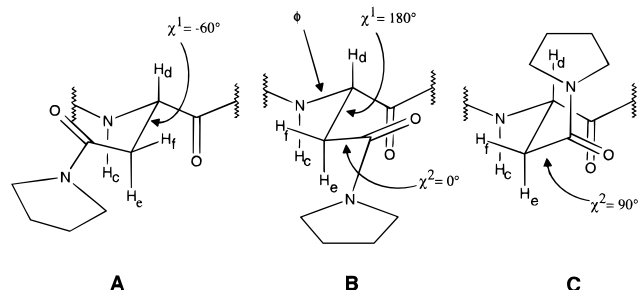
Figure 2.

relatively fixed χ^1 torsion angle. However, the data are consistent with two possibilities ($\chi^1 = -60°$ or $180°$, conformers A and B, Figure 2). The H_c-H_d coupling constants (7–8 Hz), in contrast, do not provide conclusive evidence of a fixed ϕ torsion angle. These coupling values are also typical for a conformationally mobile torsion angle. Information about the χ^2 angle is more difficult to obtain by NMR. Molecular mechanics calculations of a pyrrolidine-modified asparagine (*N*-acetyl *N*-methylamide derivative) do not find a predominant χ^2 angle. Conformers B and C shown in Figure 2 ($\chi^2 = 0°$ and $90°$, respectively) have essentially the same energy and together with conformer A constitute the three lowest energy structures found.

It was not immediately obvious how we could determine whether any of the conformations suggested by NMR and molecular modeling actually corresponded to the inhibitor bioactive conformation. However, as previously mentioned, we knew that H_c could be replaced by a methyl group with little effect on inhibitor potency. This suggested the possibility of connecting the amide nitrogen and the β-carbon by replacing H_c and H_e with a two- or three-carbon bridge. Thus, we first prepared conformationally restricted inhibitors **16** and **17** (Table 4). These two derivatives essentially lock the χ^1 angle of the pyrrolidine-modified asparagine side chain in either of the two directions suggested by the NMR data.[14] Compound **16**, which orients the side-chain carbonyl toward the inhibitor C-terminus, lost only 10 times potency compared to compound **8**, while compound **17**, which orients the side-chain carbonyl toward the inhibitor N-terminus, lost a much more substantial 1000-fold potency. These results provided the first evidence that the pyrrolidine-modified asparagine side chain prefers to be oriented toward the inhibitor C-terminus when bound to HSV R1.

The fact that compound **16** binds 10 times less effectively than compound **8** suggests that if the conformational restriction in **16** resembles the bioactive conformation, it must not be optimally orienting the local inhibitor functionality for binding. One evident disfavored orientation in compound **16** would be the χ^2 angle shown (i.e., $\chi^2 = 0°$, see conformer B, Figure 2). A steric interaction between the pyrrolidine ring and the methylenes of the conformational restriction (see highlighted bonds, compound **16**) would destabilize this conformation. The presence of the conformational restriction should not adversely affect a $90°$ χ^2 angle (see conformer C, Figure 2). To test whether this potential steric interaction had any relation to inhibitor bioactive conformation, we prepared compound **18**, a conformationally restricted inhibitor that minimizes the steric interaction when $\chi^2 = 0°$. Compound **18** turned out to be 3 times more potent than compound **16**, even though

a methylamine or ethylamine substituent usually binds 10 times less effectively than the corresponding pyrrolidine analogue (*cf.* compounds **8** and **19**, Table 4, and compounds from ref 6). This result provides strong indirect evidence that an χ^2 angle of $0°$ for the pyrrolidine-modified asparagine side chain approximates the actual angle favored for binding to R1. Significantly, compound **18** also proved 3 times more potent than the corresponding acyclic analogue, compound **19**. This observation provides more convincing evidence that the pyrrolidine-modified asparagine side chain prefers to be oriented toward the inhibitor C-terminus ($\chi^1 = 180°$).

We also investigated the 5-membered ring derivative **20**. The 5-membered ring cannot readily accommodate the χ^1 angle predicted by NMR. Thus, this derivative was prepared to verify whether the χ^1 angle predicted by NMR was in fact necessary for good inhibitor potency. As it turned out, compound **20** proved to be ca. 3 times less potent than compound **16**.

The previous results show how the conformational restrictions in compounds **16**, **18**, and **20** provide information on the side-chain bioactive conformation of the pyrrolidine-modified asparagine. We were curious whether these conformational restrictions could also provide insight into the bioactive conformation of the peptide backbone (i.e., the ϕ angle, Figure 2). This question is interesting considering that the conformational restrictions in compounds **16** and **18** lock ϕ at close to $180°$. Previous NMR data for this torsion angle indicate either conformational mobility or an angle closer to $140-150°$ ($J_{H_d-H_c} = 7-8$ Hz, Figure 2).[16] To examine the effect of the 5- and 6-membered rings on the preferred ϕ angle for binding to R1, we had to remove the side-chain carbonyl and pyrrolidine groups. Although the potency of the resulting inhibitors, compounds **21–23**, is substantially lower, the relative potency differences between compounds **21–23** are informative. The 6-membered pipecolic acid moiety in compound **21** produces an inhibitor 7 times less potent than the acyclic alanine compound **23**, while the 5-membered proline in compound **22** provides an inhibitor equipotent with **23**. These results indicate that, in contrast to the side-chain conformation, the 5-membered ring does a better job than the 6-membered ring of mimicking the preferred backbone conformation (ϕ angle) for binding to R1. Interestingly, the relevant ϕ angle in compound **20** was predicted by molecular mechanics calculations to be around $135°$. This value is close to the ϕ angle predicted by NMR coupling constants for acyclic analogues.

By combining the new information presented in this paper regarding inhibitor bioactive conformation with that previously published for the aspartic acid portion of our inhibitors, a partial picture of the overall inhibitor bioactive conformation starts to emerge. Figure 3 uses compound **8** to provide a prediction based on our conformational restrictions (dashed bonds, lower structure). At present, we do not have good direct evidence for the bioactive conformation of the important C-terminal leucine moiety. We also do not have direct evidence (via conformational restriction) for the conformational relationship between the aspartic acid moiety and the pyrrolidine-modified asparagine. However, ROESY data collected for previously published inhibitors[9] show a very strong NOE between the aspartic acid
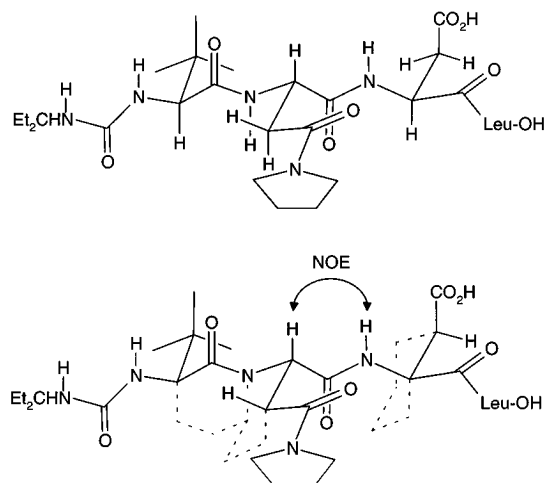
Figure 3.

NH and the asparagine Hα.[13] Although this information cannot be translated into the bioactive conformation, the strength of the NOE combined with the low-nanomolar binding potency of these inhibitors prompts us to hypothesize that these two hydrogens may also be close in the inhibitor-bound state.

From the conformation represented in Figure 3, it appears that our inhibitors bind to R1 in a predominantly extended conformation. It is also noteworthy that three bulky conformational restrictions can be incorporated into our inhibitors without dramatically decreasing binding potency. This suggests that one face of the inhibitor is primarily responsible for the interaction with R1.

Conclusion

This report reveals that introduction of an appropriately positioned NH near the inhibitor N-terminus can improve inhibitor-binding potency >50-fold over our first published inhibitor series. This NH probably takes advantage of a hydrogen-bonding interaction not used by the R2 C-terminus. We also provide evidence for the bioactive conformation around the *tert*-leucine and pyrrolidine-modified asparagine residues of our inhibitors. We obtained this evidence by correlating the structure of conformationally restricted inhibitors with inhibitor-binding potency. It appears that peptide-based inhibitors as well as the R2 C-terminus likely bind to R1 in a predominantly extended conformation.

Experimental Section

Ribonucleotide Reductase Binding Assay. The inhibitory effect of our compounds in an HSV RR radioligand binding assay was measured according to a published protocol.[17] The reported IC$_{50}$ values are the mean of at least four separate determinations, and the standard deviation from the mean is also reported.

Molecular Mechanics Calculations. The pyrrolidine-modified asparagine (*N*-acetyl *N*-methylamide derivative) was subjected to a Monte Carlo conformational search. A total of 1200 generated structures were minimized (Polak-Ribier conjugate gradient method, 2000 iterations) with the MM3 force field as implemented in MacroModel v4.0. A dielectric constant of 80 was used to lessen the contribution of intramolecular hydrogen bonds.

NMR. The NMR data that provided a basis for preparing our conformationally restricted inhibitors were obtained following the protocol in ref 9.

Scheme 1
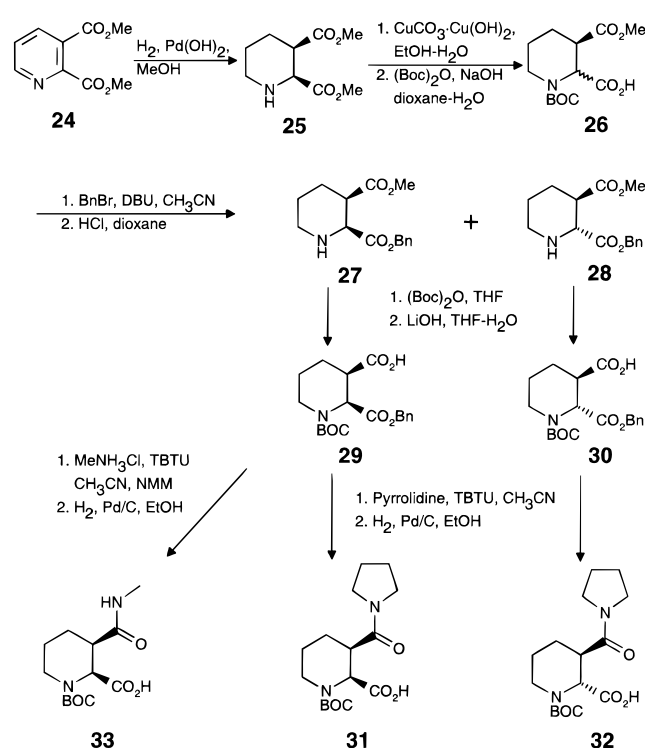
Materials. Common *N*-Boc-L-amino acids, *N*-Boc-L-*tert*-leucine, and L-leucine *O*-benzyl ester pTsOH salt were obtained from commercial sources. Boc-2(*S*)-amino-4-pyrrolidino-4-oxobutanoic acid (pyrrolidine-modified asparagine moiety) and Boc-2(*S*)-amino-4-(methylamino)-4-oxobutanoic acid (used in the preparation of inhibitor **19**) were prepared as outlined in ref 6. 3-Ethylpentanoic acid (used in the preparation of inhibitor **9**) could be prepared by the procedure in ref 18.

Synthesis of Conformationally Restricted Amino Acid Derivatives Found in Inhibitors 16−18 (Compounds 31−33). The synthesis of inhibitors **16−18** required the preparation of *N*-Boc amino acids **31−33**, respectively (Scheme 1). The synthetic sequence outlined in Scheme 1 facilitated preparation of both cis and trans isomers **31** and **32** and allowed unambiguous assignment of the structures of the products that resulted from monoester hydrolysis of the *N*-Boc derivative of intermediates **27** and **28**.[19] An alternate synthesis of compound **27** has been reported.[20] Chiral approaches to dicarboxypiperidines have been published.[19] However at the conception of this work, the achiral approach outlined in Scheme 1 was deemed expeditious.

A solution of compound **24** (45 g, 0.23 mol) in methanol (250 mL) containing 20% Pd(OH)$_2$/C (2 g) was shaken under 50 psi of H$_2$ for 16 h. Filtration and concentration provided compound **25** as a pale yellow liquid of sufficient purity for the subsequent reaction (∼46 g): ^{1}H NMR (400 MHz, CDCl$_3$) δ 3.72 (s, 3 H), 3.68 (s, 3 H), 3.63 (d, *J* = 3 Hz, 1 H), 3.05−2.97 (m, 2 H), 2.71−2.63 (m, 1 H), 2.18−2.08 (m, 1 H), 1.81−1.73 (m, 1 H), 1.51−1.46 (m, 2 H).

To a solution of diester **25** (3.0 g, 10 mmol) in ethanol (30 mL) were added water (120 mL) and CuCO$_3$·Cu(OH)$_2$ (10 g, 45 mmol). The resultant slurry was stirred at 70 °C for 22 h and then at room temperature for 16 h. H$_2$S was bubbled through the dark blue suspension (∼15 min), and the resultant black suspension was filtered through Celite (rinsing with 4:1 water−ethanol). The clear colorless filtrate was concentrated *in vacuo* to provide a white foam (∼1.9 g). This material was dissolved in water (10 mL), and 1 N aqueous NaOH (10 mL, 10 mmol), dioxane (15 mL), and a solution of Boc$_2$O (2.6 g, 12 mmol) in dioxane (5 mL) were added consecutively. The reaction mixture was stirred at room temperature for 3−5 h. Additional 1 N NaOH was added if solution pH dropped below 11. The reaction mixture was diluted with water (100 mL) and extracted with ether (2 × 50 mL). The aqueous phase

was acidified with solid citric acid and extracted with EtOAc (2 × 50 mL). The combined organic extracts were washed with brine, dried (MgSO$_4$), filtered, and concentrated to afford *N*-Boc amino acid derivative **26** as a white foam (2.5 g, 85%). Interpretation of the NMR spectrum of this material was difficult due to the mixture of diastereoisomers and rotamers present.

To a solution of **26** (2.5 g, 8.4 mmol) in dry acetonitrile (30 mL) at 0 °C were added DBU (1.26 mL, 9.2 mmol) and BnBr (1.1 mL, 9.2 mmol). The cooling bath was removed, and the reaction mixture was stirred at room temperature for 4–6 h. The solvent was remove *in vacuo*, and the residue was partitioned between EtOAc (70 mL) and saturated aqueous NaHCO$_3$ (70 mL). The organic phase was washed with water and brine, dried (MgSO$_4$), filtered, and concentrated. The resultant crude product was purified by silica gel flash chromatography (eluent, hexane–EtOAc, 4:1) to provide a clear colorless oil (2.8 g, 88%). The two diastereoisomers could not be readily separated at this stage, so the mixture was treated with 4 N HCl in dioxane (20 mL) for 30 min. The volatiles were removed *in vacuo*, and the residue was partitioned between EtOAc and saturated aqueous NaHCO$_3$. The organic phase was washed with brine, dried (MgSO$_4$), filtered, and concentrated. The two diastereoisomers could now be readily separated by silica gel flash chromatography (EtOAc eluent) to provide compounds **27** (1.2 g) and **28** (0.47 g) as colorless viscous liquids. Compound **27**: ^{1}H NMR (400 MHz, CDCl$_3$) δ 7.36–7.30 (m, 5 H), 5.21–5.15 (m, 2 H), 3.71 (d, J = 3.5 Hz, 1 H), 3.56 (s, 3 H), 3.07–2.97 (m, 2 H), 2.72–2.66 (m, 1 H), 2.20–2.10 (m, 2 H), 1.82–1.75 (m, 1 H), 1.58–1.46 (m, 2 H); FAB-MS 278 (M$^+$ + H).

Compound **28**: ^{1}H NMR (400 MHz, CDCl$_3$) δ 7.39–7.31 (m, 5 H), 5.19–5.11 (m, 2 H), 3.70 (d, J = 9 Hz, 1 H), 3.55 (s, 3 H), 3.10–3.04 (m, 1 H), 2.72–2.63 (m, 2 H), 2.06–2.01 (m, 1 H), 1.52–1.61 (m, 2 H), 1.52–1.40 (m, 1 H); FAB-MS 278 (M$^+$ + H). The two coupling constants reported for compounds **27** and **28** (NC*H*CO$_2$) were consistent with the relative stereochemistries shown.

To a solution of compound **27** or **28** (1.7 mmol) in THF (5 mL) was added Boc$_2$O (2 mmol), and the resultant mixture was stirred at room temperature for 16 h. The reaction mixture was concentrated and the residue purified by flash chromatography (eluent, hexane–EtOAc, 4:1) to provide clear colorless oils in essentially quantitative yield. To a solution of this oil (1.7 mmol) in 3:1 THF–water (13 mL) was added a solution of aqueous LiOH (1 N, 2 mL, 2 mmol) dropwise at a rate to maintain a clear homogeneous reaction mixture. After complete addition, the reaction mixture was stirred at room temperature for 1–2 h, diluted with water (60 mL), and extracted with ether to remove any unreacted starting material. The aqueous phase was acidified to pH ~2 with 0.5 N aqueous HCl and extracted with EtOAc (2 × 50 mL). The combined organic extracts were washed with brine, dried (MgSO$_4$), filtered, and concentrated to provide compound **29** or **30** as a sticky solid (~1 mmol, each product was contaminated with material resulting from benzyl ester hydrolysis). NMR of this material was complex (rotamers); however, it indicated that methyl ester hydrolysis was favored over benzyl ester hydrolysis by ca. 2:1. Crude **29** or **30** was subjected to amide bond formation with either pyrrolidine or methylamine hydrochloride by using the typical coupling procedure outlined in Inhibitor Synthesis. In each case, the desired isomer could be isolated pure by flash chromatography (~20–30% yield from compound **27** or **28**).

The pure benzyl ester derivative (0.5 mmol) was mixed with methanol (5 mL) and 10% Pd/C (50 mg) and stirred under 1 atm of H$_2$ for 1–2 h. The reaction mixture was filtered and concentrated to provide *N*-Boc amino acid derivatives **31** and **32** as white foams. These compounds were of sufficient purity for coupling to β-benzyl-L-aspartic acid L-leucine *O*-benzyl ester. Analytical samples could be obtained by reverse phase HPLC (Whatman Partisil 10 ODS-3 column, eluent 0–60% acetonitrile in water, both solvents containing 0.06% TFA) followed by lyophilization. Compound **31**: ^{1}H NMR (400 MHz, CDCl$_3$), spectrum shows a 65:35 mixture of rotamers, δ 5.48–5.44 (br, 0.65 H), 5.28–5.22 (br, 0.35 H), 4.02–3.84 (br m, 1

Scheme 2
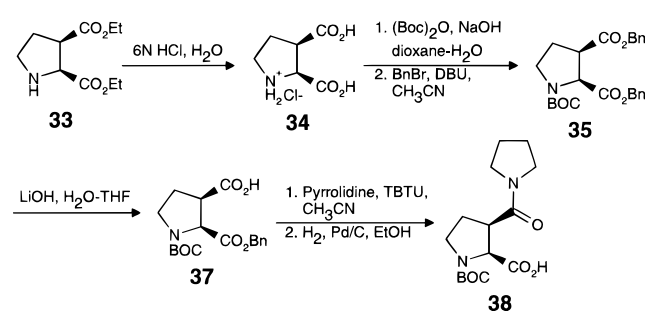
H), 3.67–3.30 (br m, 4 H), 2.83–2.30 (br m, 3 H), 2.08–1.40 (br m, 7 H), 1.46 (s, 9 H); FAB-MS 327 (M$^+$ + H).

Compound **32**: ^{1}H NMR (400 MHz, CDCl$_3$) δ 4.97–4.91 (br, 1 H), 3.84–3.12 (br m, 7 H), 2.05–1.64 (m, 8 H), 1.47 (s, 9 H); FAB-MS 327 (M$^+$ + H).

Compound **33**: ^{1}H NMR (400 MHz, DMSO-d_6), spectrum shows a 65:35 mixture of rotamers, δ 8.43–8.38 (br, 0.35 H), 7.87–7.80 (br, 0.65), 5.01–4.97 (br, 0.65 H), 4.89–4.85 (br, 0.35 H), 4.05–4.00 (br, 0.35 H), 3.83–3.74 (br, 0.65 H), 3.3–2.38 (br m, 3 H, overlaps with DMSO and H$_2$O), 2.60 (br d, J = 3.5 Hz, 1.05 H), 2.57 (br d, J = 4 Hz, 1.95 H), 2.01–1.30 (m, 3 H), 1.39 (br s, 9 H); FAB-MS 287 (M$^+$ + H).

**Synthesis of the Conformationally Restricted Amino Acid Derivative Found in Inhibitor 20 (Compound 38).** The synthesis of *N*-Boc amino acid **38** started from diethyl *cis*-2,3-pyrrolidinedicarboxylate (**33**)[21] (Scheme 2). A solution of **33** (1.67 g, 7.76 mmol) in 6 N aqueous HCl (13 mL) was refluxed for 22 h. The reaction mixture which contained a fine black precipitate was filtered through a 4 μm Milex filter unit. Concentration of the filtrate and drying *in vacuo* provided a yellow solid (1.48 g, 97%) which was used in the next reaction without further purification:[22] ^{1}H NMR (400 MHz, DMSO-d_6) δ 4.43 (d, J = 7 Hz, 1 H), 3.45 (ddd, J = 8, 3.5, 3 Hz, 1 H), 3.28–3.23 (m, 2 H), 2.35–2.25 (m, 1 H), 2.19–2.11 (m, 1 H); FAB-MS 244 (M$^+$ + H).

Amino acid **34** was converted to *N*-Boc dibenzyl ester derivative **35** by using procedures similar to those described above (two of the reactions used in conversion of **25** to **27**). An extra 1 equiv of NaOH was required for the *N*-Boc reaction, and an extra 1 equiv each of DBU and BnBr was used for the benzylation reaction. Compound **35** was isolated as a clear colorless liquid: ^{1}H NMR (400 MHz, CDCl$_3$), spectrum shows a 65:35 mixture of rotamers, δ 7.35–7.20 (m, 10 H), 5.11–4.89 (m, 3.65 H), 4.77 (d, J = 12 Hz, 0.35 H), 4.69 (d, J = 8.5 Hz, 0.35 H), 4.55 (d, J = 8.5 Hz, 0.65 H), 3.78–3.65 (m, 1 H), 3.44–3.25 (m, 2 H), 2.48–2.36 (m, 1 H), 2.19–2.08 (m, 1 H), 1.45 (s, 3.15 H), 1.33 (s, 5.85 H); FAB-MS 440 (M$^+$ + H).

To a solution of **35** (2.83 g, 6.45 mmol) in 3:1 THF–H$_2$O (65 mL) was added 1 N aqueous LiOH (7.8 mL, 7.8 mmol) at a rate to maintain reaction homogeneity. After 2 h, the reaction mixture was diluted with water (150 mL) and extracted with ether (2 × 100 mL). The aqueous phase was acidified to pH 2–3 with 1 N aqueous HCl and extracted with EtOAc (2 × 70 mL). The combined organic extracts were dried (MgSO$_4$), filtered, and concentrated to afford a white solid (1.6 g, NMR shows a mixture of isomers). This material could be crystallized from 5:1 heptane–EtOAc to provide **37** as fine needles (0.8 g, 35%): mp 131–132 °C; ^{1}H NMR (400 MHz, CDCl$_3$), spectrum shows a 65:35 mixture of rotamers, δ 7.34–7.29 (m, 5 H), 5.18–5.04 (m, 2 H), 4.69 (d, J = 8.5 Hz, 1 H), 4.57 (d, J = 8.5 Hz, 1 H), 3.78–3.64 (m, 1 H), 3.46–3.24 (m, 2 H), 2.44–2.33 (m, 1 H), 2.19–2.08 (m, 1 H), 1.46 (s, 3.15 H), 1.33 (s, 5.85 H); FAB-MS 350 (M$^+$ + H). Anal. Calcd for C$_{18}$H$_{23}$NO$_6$: C, 61.88; H, 6.64; N, 4.01. Found: C, 61.80; H, 6.64; N, 3.94. Proof of structure was obtained by X-ray crystallography (structure available as Supporting Information).

Compound **37** was converted to the *N*-Boc amino acid derivative **38** as described for compounds **31**–**33**. Compound **38** was obtained as a white foam (93% yield): ^{1}H NMR (400 MHz, CDCl$_3$), spectrum shows a 60:40 mixture of rotamers, δ 4.62–4.58 (m, 0.4 H), 4.43 (br d, J = 7.5 Hz, 0.6 H), 3.83–

Scheme 3
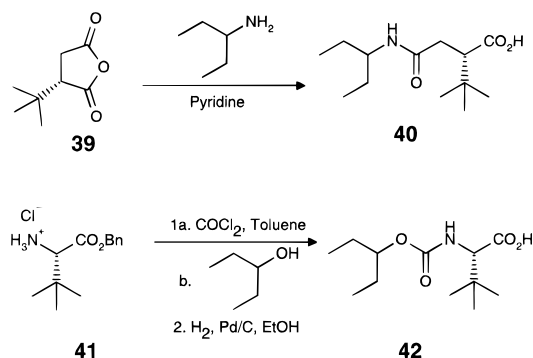
Scheme 4

3.29 (br m, 7 H), 2.62−2.50 (br m, 1 H), 2.05−1.81 (br m, 5 H), 1.48 (s, 3.6 H), 1.43 (s, 5.4 H); FAB-MS 312 (M^+ + H).

Preparation of the *tert*-Butylsuccinoyl Moiety Found in Inhibitor 11 (Compound 40). Scheme 3 outlines the preparation of compound **40**. To a solution of (*R*)-*tert*-butyl-succinic anhydride[23] (**39**) (50 g, 0.32 mol) in dry pyridine (1.2 L) at −40 °C was added a solution of 3-aminopentane (33.5 g, 0.38 mol) in pyridine (0.1 L). The reaction mixture was allowed to warm to room temperature and stirred for 16 h. Volatiles were removed under aspirator vacuum (50 °C), and the residue was dissolved in EtOAc (500 mL). This solution was washed with 20% citric acid (4 × 100 mL) and brine (2 × 100 mL), dried (MgSO$_4$), filtered, and concentrated to provide a colorless liquid. This material was dissolved in 3:1 hexane−ether (400 mL) (warming required) and allowed to crystallize for 4 h at room temperature and then for 12 h at 5 °C. Filtration and washing with 10% ether in hexane provided compound **40** as a white solid (58.5 g, 75%): mp 124−127 °C; [α]$^{23}_D$ −7.5° (*c* 1.00, CHCl$_3$); ^{1}H NMR (400 MHz, CDCl$_3$) δ 5.40 (d, *J* = 9 Hz, 1 H), 3.79−3.70 (m, 1 H), 2.78 (dd, *J* = 11.5, 3.5 Hz, 1 H), 2.53 (dd, *J* = 14.5, 11.5 Hz, 1 H), 2.41 (dd, *J* = 14.5, 3.5 Hz, 1 H), 1.58−1.45 (m, 2 H), 1.40−1.28 (m, 2 H), 1.02 (s, 9 H), 0.87 (t, *J* = 7.5 Hz, 3 H), 0.85 (t, *J* = 7.5 Hz, 3 H); FAB-MS 244 (M^+ + H). Anal. Calcd for C$_{13}$H$_{25}$NO$_3$: C, 64.17; H, 10.36; N, 5.76. Found: C, 63.99; H, 10.54; N, 5.70.

Preparation of Carbamate N-Terminus Found in Inhibitor 10 (Compound 42). Scheme 3 outlines the preparation of compound **42**. L-*tert*-Leucine *O*-benzyl ester hydrochloride salt (**41**) (92 mg, 0.42 mmol) was treated with a commercially available solution of phosgene in toluene (1.93 M, 4 mL). The suspension was refluxed (dry ice condenser) for 1 h, after which time excess phosgene was removed by bubbling nitrogen through the reaction solution. 3-Pentanol (180 μL, 1.65 mmol) was added to the isocyanate solution, and the resultant mixture was stirred at 95 °C for 3 h. The reaction mixture was diluted with EtOAc (20 mL) and washed with saturated aqueous sodium bicarbonate and brine. Drying (MgSO$_4$), filtering, and concentrating afforded a thick colorless liquid (90 mg). This material was mixed with ethanol (6 mL) and 10% Pd/C (5 mg) and stirred under an atmosphere of H$_2$ for 2 h. Filtration and concentration provided compound **42** as a thick oil in sufficient purity for the subsequent coupling reaction (65 mg): ^{1}H NMR (400 MHz, DMSO-d_6) δ 7.07 (d, *J* = 9 Hz, 1 H), 4.55−4.44 (m, 1 H), 3.83 (d, *J* = 9 Hz, 1 H), 1.56−1.42 (m, 4 H), 0.76 (s, 9 H), 0.86−0.80 (m, 3 H); FAB-MS 246 (M^+ + H).

Preparation of Inhibitors 13 and 14. The synthesis of compounds **13** and **14** relied on the preparation of aldehyde derivatives **44** and **45**,[25] respectively (Scheme 4). The successful reductive amination of compound **44** required the α-amino group to be diprotected.[26] *N*-Cbz-β-allyl-D-aspartic acid *tert*-butyl ester, available by standard amino acid protection reactions, was converted to compound **43** by the following procedure. To a solution of the former (1.67 g, 4.43 mmol) in CH$_3$CN (10 mL) were added Boc$_2$O (1.06 g, 4.87 mmol) and DMAP (54 mg, 0.44 mmol). The reaction mixture was stirred at room temperature for 16 h, after which time the solvent was evaporated and the residue partitioned between EtOAc and saturated aqueous NaHCO$_3$. The organic phase was
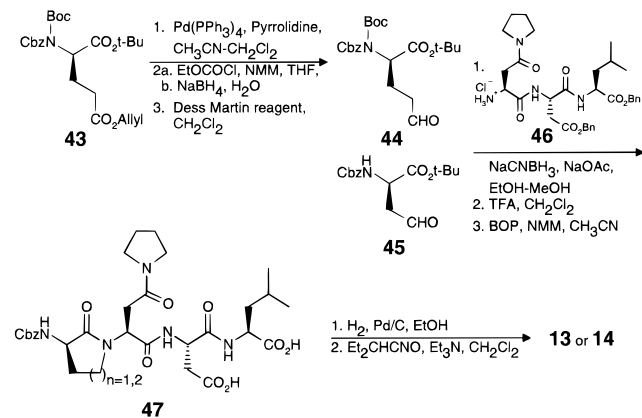
washed with brine, dried (MgSO$_4$), filtered, and concentrated. The crude product was purified by silica gel flash chromatography (hexane−EtOAc, 10:1) to provide **43** as a clear viscous liquid (1.78 g, 84%): ^{1}H NMR (400 MHz, CDCl$_3$) δ 7.40−7.28 (m, 5 H), 5.95−5.82 (m, 1 H), 5.33−5.16 (m, 4 H), 4.87 (dd, *J* = 9, 4 Hz, 1 H), 4.57−4.53 (m, 2 H), 2.49−2.32 (m, 3 H), 2.23−2.13 (m, 1 H), 1.45 (s, 9 H), 1.39 (s, 9 H).

Compound **43** was converted to compound **44** by established procedures: deallylation,[27] reduction of the acid to the alcohol,[26] and oxidation.[28] Compound **44**: ^{1}H NMR (400 MHz, CDCl$_3$) δ 9.71 (s, 1 H), 7.41−7.30 (m, 5 H), 5.28 (d, *J* = 13 Hz, 1 H), 5.20 (d, *J* = 13 Hz, 1 H), 4.82 (dd, *J* = 8.5, 4 Hz, 1 H), 2.60−2.41 (m, 3 H), 2.22−2.12 (m, 1 H), 1.45 (s, 9 H), 1.39 (s, 9 H).

To a solution of tripeptide salt **46** (0.5 mmol) in EtOH (7 mL) were added a solution of aldehyde **44** or **45** (0.5 mmol) in MeOH (3 mL) and solid NaOAc to adjust pH to ~5. The resultant mixture was cooled to 0 °C, and NaCNBH$_3$ (0.6 mmol) was added in three portions over 15 min. The reaction mixture was stirred at room temperature for 3 h, the solvent was evaporated, and the residue was partitioned between EtOAc and brine. The organic phase was washed with brine, dried (MgSO$_4$), filtered, and concentrated. The crude reductive amination product was purified by silica gel flash chromatography to provide white foams (50−80%). This material was treated with a 1:1 mixture of TFA and dichloromethane (10 mL) for 1 h. The volatiles were removed *in vacuo*, and the residue was dissolved in acetonitrile (10 mL). NMM (3 equiv) and BOP reagent (1 equiv) were added, and the reaction mixture was stirred at room temperature for 1 h. The solvent was evaporated, and the residue was partitioned between EtOAc and saturated aqueous NaHCO$_3$. The organic phase was washed with 1 N HCl and brine, dried (MgSO$_4$), filtered, and concentrated. The crude products were purified by silica gel flash chromatography to provide compounds **47** as white foams (80−85%). Compounds **47** (0.2 mmol) were mixed with 1:1 THF−MeOH (10 mL) and 10% Pd/C (50 mg) and stirred under an atmosphere of H$_2$ for 2 h. The reaction mixture was filtered and concentrated, and the residue was dissolved/suspended in dry dichloromethane (10 mL). Triethylamine (0.7 mmol) and 1-ethylpropyl isocyanate (0.7 mmol) were added, and the resultant mixture was stirred at room temperature for 16 h, after which time the volatiles were removed *in vacuo*. The residue was dissolved in water (~5 mL), and the resultant solution was acidified to pH 4 with 1 N HCl. This solution was passed through a preparative HPLC C18 reverse phase column (Vydac, 15 μm particle size) eluting with a 0.06% aqueous TFA−0.06% TFA in acetonitrile gradient (0−43% acetonitrile) to provide, after concentration and lyophilization of the appropriate fractions, compounds **13** and **14** as fluffy white solids (50−80%). Full characterization of these compounds is provided in the Supporting Information.

Inhibitor Synthesis. All inhibitors were prepared by solution phase peptide synthesis, in which *N*-Boc-amino acid derivatives were coupled sequentially from C- to N-terminus by using benzotriazol-1-yl-1,1,3,3-tetramethyluronium tetrafluoroborate (TBTU) as the coupling agent. Removal of the

N-Boc protective group was effected with 4 N HCl in dioxane. The following procedure is representative. To a solution of *N*-Boc-amino acid (1 mmol) in dry acetonitrile (2.5 mL) were added TBTU (1 mmol) and *N*-methylmorpholine (1 mmol). After ca. 5 min, this solution was added to a solution of L-leucine *O*-benzyl ester pTsOH salt or peptide hydrochloride salt (1 mmol) in dry acetonitrile (2.5 mL) containing *N*-methylmorpholine (2 mmol). The reaction mixture was stirred at ambient temperature for 2−6 h (reaction monitored by TLC) and then poured into a mixture of EtOAc (50 mL) and saturated aqueous sodium bicarbonate (50 mL). The organic phase was washed with another portion of sodium bicarbonate, 1 N aqueous HCl (2 × 50 mL), and brine (50 mL). Drying (MgSO$_4$), filtration, and concentration provided the peptide, usually of sufficient purity to continue to the next step without further purification. *N*-Boc peptide derivatives could be purified if necessary by conventional flash chromatography. The *N*-Boc peptide product (1 mmol) was then treated with 4 N HCl in dioxane (5 mL) for 30 min. The solvent was removed under vacuum, and the resulting hydrochloride salt was subjected to high vacuum before its use in the next coupling reaction.

The conformationally restricted amino acid derivatives **31**−**33** and **38** used in the preparation of inhibitors **16**−**18** and **20,** respectively, were incorporated as racemates. The diastereoisomers obtained on coupling these racemic amino acid derivatives with β-benzyl-L-aspartic acid L-leucine *O*-benzyl ester were readily separated by flash chromatography. Both diastereoisomers were elaborated to the corresponding final peptide, and in each case, one of the diastereoisomers proved to have inhibitory activity at least 100−1000 times greater than the other (potency differences affected by traces of contaminating active isomer). For compounds **31**−**33**, the first diastereoisomer to elute provided the most potent inhibitor, while for compound **38**, the bottom isomer provided the most potent inhibitor. The configuration of the active diastereoisomer was assigned as corresponding to L based on precedent with other active inhibitors containing L-asparagine derivatives (e.g., compounds **8** and **19**) and the fact that a previously made peptide inhibitor containing D-asparagine had significantly reduced inhibitory activity.[12]

The various N-terminal alkylureido functionalities were introduced as follows. To a solution of the appropriate peptide hydrochloride salt (0.5 mmol) in dry dichloromethane (5 mL) were added *N*-methylmorpholine (1.5 mmol) and the relevant isocyanate (1 mmol, usually neat). The reaction mixture was stirred at room temperature for 16 h, after which time the volatiles were removed and the residue was partitioned between EtOAc and 0.1 M aqueous HCl. The organic phase was washed with 5% aqueous sodium bicarbonate and brine, dried (MgSO$_4$), filtered, and concentrated. The resultant crude product was purified by silica gel flash chromatography to provide the desired ureido derivatives usually as white foams (64−76% yield). Isopropyl and methyl isocyanates were obtained from commercial sources. 1-Propylbutyl and 1-ethylpropyl isocyanates were prepared from commercially available 4-aminoheptane and 3-aminopentane, respectively, by following the procedure in ref 24.

The last reaction involved in the preparation of our inhibitors involved removal of the two benzyl ester protective groups by catalytic hydrogenolysis (10 mol % 10% Pd/C in methanol under 1 atm of H$_2$ for 3 h). The resultant inhibitor was often obtained in >95% purity (HPLC and NMR), but when necessary it was purified by preparative HPLC on a C18 reverse phase column (Vydac, 15 μm particle size) eluting with 0.06% aqueous TFA−0.06% TFA in acetonitrile gradients.

Inhibitor Characterization and Purity. All peptide derivatives showed satisfactory 400 MHz ^{1}H NMR spectra, FAB mass spectra (M$^+$ + H) and/or (M$^+$ + Na), amino acid analysis including peptide recovery, and HPLC purity in two solvent systems (>95%).

Supporting Information Available: Full tabulation of ^{1}H NMR, FAB mass spectra, amino acid analysis, elemental analysis, and HPLC purity data for new inhibitors and the X-ray structure of compound **37** (16 pages). Ordering information is given on any current masthead page.

References

(1) Cory, J. G. Role of ribonucleotide reductase in cell division. In *Inhibitors of Ribonucleoside Diphosphate Reductase Activity*; Cory, J. G., Cory, A. H., Eds.; Pergamon Press Inc.: New York, 1989; pp 1−17.

(2) Filatov, D.; Ingemarson, R.; Graslund, A.; Thelander, L. The role of herpes simplex virus ribonucleotide reductase small subunit carboxyl terminus in subunit interaction and formation of iron-tyrosyl center structure. *J. Biol. Chem.* **1992**, *267*, 15816−15822.

(3) (a) Dutia, B. M.; Frame, M. C.; Subak-Sharpe, J. H.; Clarke, W. N.; Marsden, H. S. Specific inhibition of herpes virus ribonucleotide reductase by synthetic peptides. *Nature* **1986**, *321*, 439−441. (b) Cohen, E. A.; Gaudreau, P.; Brazeau, P.; Langelier, Y. Specific inhibition of herpes simplex virus ribonucleotide reductase activity by a nonapeptide derived from the carboxyl terminus of subunit 2. *Nature* **1986**, *321*, 441−443.

(4) Cosentino, G.; Lavallée, P.; Rakhit, S.; Plante, R.; Gaudette, Y.; Lawetz, C.; Whitehead, P. W.; Duceppe, J.-S.; Lépine-Frenette, C.; Dansereau, N.; Guilbault, C.; Langelier, Y.; Gaudreau, P.; Thelander, L.; Guindon, Y. Specific inhibition of ribonucleotide reductases by peptides corresponding to the C-terminal of their second subunit. *Biochem. Cell Biol.* **1991**, *69*, 79−83.

(5) Liuzzi, M.; Déziel, R.; Moss, N.; Beaulieu, P.; Bonneau, A.-M.; Bousquet, C.; Chafouleas, J. G.; Garneau, M.; Jaramillo, J.; Krogsrud, R. L.; Lagacé, L.; McCollum, R. S.; Nawoot, S.; Guindon, Y. A potent peptidomimetic inhibitor of HSV ribonucleotide reductase with antiviral activity *in vivo. Nature* **1994**, *372*, 695−698.

(6) Moss, N.; Déziel, R.; Adams, J.; Aubry, N.; Bailey, M.; Baillet, M.; Beaulieu, P.; DiMaio, J.; Duceppe, J.-S.; Ferland, J.-M.; Gauthier, J.; Ghiro, E.; Goulet, S.; Grenier, L.; Lavallée, P.; Lépine-Frenette, C.; Plante, R.; Rakhit, S.; Soucy, F.; Wernic, D.; Guindon, Y. Inhibition of herpes simplex virus type 1 ribonucleotide reductase by substituted tetrapeptide derivatives. *J. Med. Chem.* **1993**, *36*, 3005−3009.

(7) Ulin, U.; Eklund, H. Structure of ribonucleotide reductase protein R1. *Nature* **1994**, *370*, 533−539.

(8) Bushweller, J. H.; Bartlett, P. A. Investigation of an octapeptide inhibitor of escherichia coli ribonucleotide reductase by transferred nuclear Overhauser effect spectroscopy. *Biochemistry* **1991**, *30*, 8144−8150.

(9) Moss, N.; Déziel, R.; Ferland, J.-M.; Goulet, S.; Jones, P.-J.; Leonard, S. F.; Pitner, T. P.; Plante, R. Herpes simplex virus ribonucleotide reductase subunit association inhibitors: the effect and conformation of β-alkylated aspartic acid derivatives. *Bioorg. Med. Chem.* **1994**, *2*, 959−970.

(10) Gaudreau, P.; Paradis, H.; Langelier, Y.; Brazeau, P. Synthesis and inhibitory potency of peptides corresponding to the subunit 2 C-terminal region of herpes virus ribonucleotide reductase. *J. Med. Chem.* **1990**, *33*, 723−730.

(11) Moss, N.; Beaulieu, P.; Duceppe, J.-S.; Ferland, J.-M.; Gauthier, J.; Ghiro, E.; Goulet, S.; Grenier, L.; Llinas-Brunet, M.; Plante, R.; Wernic, D.; Déziel, R. Peptidomimetic inhibitors of HSV ribonucleotide reductase: a new class of antiviral agents. *J. Med. Chem.* **1995**, *38*, 2723−2730.

(12) Chou, P. Y.; Fasman, D. G. Prediction of the secondary structure of proteins from their amino acid sequence. *Adv. Enzymol.* **1978**, *47*, 45−148.

(13) A full account of the NMR-derived solution structure of these compounds and others will be published separately.

(14) Unpublished observation.

(15) Even though the restricted amino acid derivative in compound **17** contains two substituents in the axial position on the piperidine ring, the conformation shown predominates in solution (4.5−5 Hz). Substantial A^{1,3} strain between the two backbone amides likely destabilizes the alternate chair form. A slight twisting of the chair conformations shown for compounds **16**−**18** may exist, but this should not invalidate the general conclusions made.

(16) Pardi, J.; Billeter, M.; Wüthrich, K. Calibration of the angular dependence of the amide proton-Cα proton coupling constants in a globular protein. *J. Mol. Biol.* **1984**, *180*, 741−751.

(17) Krogsrud, R. L.; Welchner, E.; Scouten, E.; Liuzzi, M. A solid-phase assay for the binding of peptidic subunit association inhibitors to the herpes simplex virus ribonucleotide reductase large subunit. *Anal. Biochem.* **1993**, *213*, 386−390.

(18) Kepner, R. E.; Winstein, S.; Young, W. G. Allylic rearrangements. XXIV. Abnormal bimolecular substitution. The condensation of butenyl and pentenyl chlorides with sodium malonic ester. *J. Am. Chem. Soc.* **1949**, *71*, 114−119.

(19) Monoester hydrolysis of related derivatives is known to be nonselective. Gmeiner, P.; Feldman, P. L.; Chu-Moyer, M. Y.; Rapoport, H. An efficient and practical total synthesis of (+)-vicamine from *L*-aspartic acid. *J. Org. Chem.* **1990**, *55*, 3068−3074.

(20) Johansen, J. E.; Christie, B. D.; Rapoport, H. Iminium salts from α-aminoacid decarbonylation. Application to the synthesis of octahydroindolo[2,3-a]quinolizines. *J. Org. Chem.* **1981**, *46*, 4914−4920.

(21) Röder, E.; Wiedenfeld, H.; Bourauel, T. Synthese von 2,3-Bis-(ethoxycarbonyl)-1*H*-pyrrol-1-propionsäure-ethylester. *Liebigs Ann. Chem.* **1987**, 1117−1119.

(22) A chiral synthesis of the neutral amino acid of compound **34** has been reported. Humphrey, J. M.; Bridges, R. J.; Hart, J. A.; Chamberlin, A. R. 2,3-Pyrrolidinedicarboxylates as neurotransmitter conformer mimics: enantioselective synthesis via chelation-controlled enolate alkylation. *J. Org. Chem.* **1994**, *59*, 2469−2472.

(23) Polonski, T. Chiroptical properties and molecular geometry of substituted succinic anhydrides and imides. *J. Chem. Soc. Perkin Trans. 1* **1988**, 629−637.

(24) Goldesmidt, V. S.; Wick, M. Über peptid-synthesen I. *Liebigs Ann. Chem.* **1952**, *575*, 217−231.

(25) Valerio, R. M.; Alewood, P. F.; Johns, R. B. Synthesis of optically active 2-(*tert*-butoxycarbonylamino)-4-dialkyloxyphosphorylbutanoate protected isosteres of *O*-phosphonoserine for peptide synthesis. *Synthesis* **1988**, 786−789.

(26) Zydowsky, T. M.; Dellaria, J. F.; Nellans, H. N. Efficient and versatile synthesis of dipeptide isosteres containing γ- or δ-lactams. *J. Org. Chem.* **1988**, *53*, 5607−5616.

(27) Déziel, R. Mild palladium(0)-catalyzed deprotection of allyl esters. A useful application in the synthesis of carbapenems and other β-lactam derivatives. *Tetrahedron Lett.* **1987**, *28*, 4371−4372.

(28) Dess, D. B.; Martin, J. C. Readily accessible 12-I-5 oxidant for the conversion of primary and secondary alcohols to aldehydes and ketones. *J. Org. Chem.* **1983**, *48*, 4155−4156.